# $\eta^1$ versus $\eta^5$ Bonding Modes in Cp*Al(I) Adducts of 9-Borafluorenes

Patricio E. Romero,[†] Warren E. Piers,*[,†] Stephen A. Decker,[‡] Dan Chau,[‡] Tom K. Woo,*[,‡] and Masood Parvez[†]

*Department of Chemistry, University of Calgary, 2500 University Drive, N.W., Calgary, Alberta, Canada, T2N 1N4, and Department of Chemistry, University of Western Ontario, London, Ontario, Canada, N6A 5B7*

*Received December 10, 2002*

The reactivity of highly Lewis acidic perfluorinated borafluorenes $C_{12}F_8BR$ (R = $C_6F_5$, **1a**; $CH_3$, **1b**) and the nonfluorinated 9-phenyl-9-borafluorene (**2**) toward $[Cp^*Al]_4$ was investigated. The reaction of **1** with $[Cp^*Al]_4$ leads to the formation of thermally robust $\eta^1$ Lewis acid−base adducts **3a**,**b** as the thermodynamically favored products. Use of the less Lewis acidic **2** does not alter the mode of reactivity, with the $\eta^1$ Lewis acid−base **4** formed preferentially. Reduction of **2** to the 9-boratafluorene **2**·$Li_2(THF)_n$ is readily accomplished in THF solution. However, reaction of **2**·$Li_2(THF)_n$ with $[Cp^*AlCl_2]_2$ or $Cp^*AlCl_2(THF)$, **5**, affords aluminum metal, **2**·THF, and Cp*H as the main identifiable products. Compounds **3a**, **3b**, **4**, and **5** were fully characterized including their X-ray structures. A DFT computational study was conducted to probe the reason for the strong preference for $\eta^1$ bonding, which essentially stems from the localization of aromaticity in the flanking phenyl rings in the 9-borafluorene ring system.

## Introduction

Boron-containing rings, such as borabenzenes,[1] boratabenzenes,[2] and boroles,[3] are a versatile class of ligands for transition metals since they are isoelectronic to the ubiquitous cyclopentadienyl (Cp) ancillary. Unlike Cp ligands, however, the reactivity of complexes bearing the boron-based donors, particularly boratabenzenes and borollides, can be finely adjusted via variation of the substituent on boron. Thus, while providing steric coverage similar to the Cp anion, the range of electronic variation possible is significantly wider. This feature has been exploited most elegantly within the context of olefin polymerization catalysis by metallocene mimics containing these ligands.[3k,4]

**Chart 1**

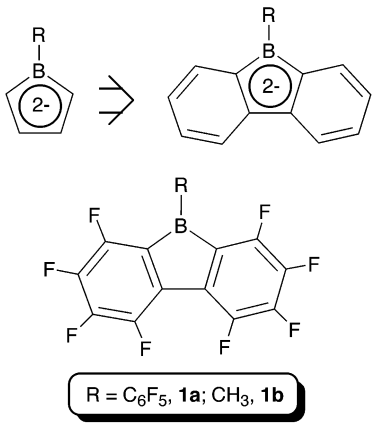


While boron-containing heterocycles have found utility as $Cp^-$ replacements, such analogues of benzannulated Cp donors, like the indenyl ligand,[5] are less common. Similarly, the dianions of 9-borafluorenes, which would be dianionic replacements for the fluorenyl donor,[6] are a relatively unexplored class of boracyclic ligands (Chart 1). These benzannulated structural relatives of boroles have been known since an early report by Köster and Benedict in 1963,[7] but reports of their

* Corresponding author: S. Robert Blair Professor of Chemistry (2000−2005); E.W.R. Steacie Memorial Fellow (2000−2002). Phone: (403) 220-5746. Fax: (403) 289-9488. E-mail: wpiers@ucalgary.ca.

† University of Calgary.

‡ University of Western Ontario.

(1) (a) Nöth, H.; Schmidt M. *Angew. Chem., Int. Ed. Engl.* **1996**, *35*, 292. (b) Hoic, D. A.; Davis W. M., Fu G. C. *J. Am. Chem. Soc.* **1995**, *117*, 8480. (c) Boese, R.; Finke, N.; Henkelmann J.; Maier G.; Paetzold, P.; Reisenahuer, H. P.; Schmid, G. *Chem. Ber.* **1985**, *118*, 1644. (d) Hoic, D. A.; Wolf, J. R.; Davis, W. M.; Fu, G. C. *Organometallics* **1996**, *15*, 1315.

(2) (a) Service, R. F. *Science* **1996**, *271*, 1363. (b) Bazan, G. C.; Rodriguez, G.; Ashe, A. J., III; Al-Ahmad, S.; Muller, C. *J. Am. Chem. Soc.* **1996**, *118*, 2291. (c) Herberich, G. E.; Ohst H. *Adv. Organomet. Chem.* **1986**, *25*, 199.

(3) (a) Herberich, G. E. Boron Rings Ligated to Metals. In *Comprehensive Organometallic Chemistry II*; Stone, E. W., Wilkinson, F. G. A., Eds.; Pergamon Press: Oxford, 1995; p 197. (b) Eisch, J. J.; Galle, J. E.; Kozima S. *J. Am. Chem. Soc.* **1986**, *108*, 379. (c) Pindado, G.; Lancaster, S. J.; Thornton-Pett, M.; Bochmann, M. *J. Am. Chem. Soc.* **1998**, *120*, 6816. (d) Herberich, G. E.; Eckenrath, H. J.; Englert, U. *Organometallics* **1997**, *16*, 4800. (e) Herberich, G. E.; Eckenrath, H. J.; Englert, U. *Organometallics* **1997**, *16*, 4292. (f) Braunstein, P.; Herberich, G. E.; Neuschutz, M.; Schmidt, M. U.; Englert, U.; Lecante, P.; Mosset, A. *Organometallics* **1998**, *17*, 2177. (g) Herberich, G. E.; Eckenrath, H. J.; Englert, U. *Organometallics* **1998**, *17*, 519. (h) Woodman, T. J.; Thornton-Pett, M.; Hughes, D. L.; Bochmann, M. *Organometallics* **2001**, *20*, 4080. (i) Woodman, T. J.; Thornton-Pett M.; Bochmann, M. *Chem. Commun.* **2001**, 329. (j) Braunstein, P.; Englert, U.; Herberich, G. E.; Neuschutz, M.; Schmidt, M. U. *J. Chem. Soc., Dalton Trans.* **1999**, 2807. (k) Sperry, C. K.; Cotter, W. D.; Lee, R. A.; Lachicotte, R. J.; Bazan, G. C. *J. Am. Chem. Soc.* **1998**, *120*, 7791.

(4) (a) Herberich, G. E.; Ohst, H. *Naturforsch.* **1983**, *B38*, 1388. (b) Quan, R. W.; Bazan, G. C.; Schaefer, W. P.; Bercaw, J. E.; Kiely, A. F. *J. Am. Chem. Soc.* **1994**, *116*, 4489, and references therein.

(5) Ashe, A. J., III; Yang, H.; Fang, X.; Kampf, J. W. *Organometallics* **2002**, *21*, 4578.

(6) Alt, H. G.; Samuel, E. *Chem. Soc. Rev.* **1998**, *27*, 323.

10.1021/om0209935 CCC: $25.00 
Publication on Web 02/19/2003

use as dianionic ligands are absent from the literature. Like boroles, 9-borafluorenes are stronger Lewis acids[8] than acyclic analogues and are readily reduced to their corresponding dianions by treatment with an appropriate reducing agent in polar solvents. Power[9] and Wehmschulte[10] have recently reported examples of this process, and the dianionic boratafluorene species have been structurally characterized. Despite the availability of these synthons, attempts to ligate to a transition metal have been characterized by facile reduction processes, which resulted in recovery of the neutral 9-borafluorene precursor.

We have recently reported the synthesis and characterization of the novel, highly fluorinated 9-borafluorenes **1** (R = $C_6F_5$, **1a**; R = $CH_3$, **1b**), powerful Lewis acids that serve as effective activators for group 4 metallocene polymerization catalyst precursors.[11] In addition to their use as Lewis acid activators, we were interested in probing their capacity for use as dianionic, but potentially electron-deficient ligands. Unlike nonfluorinated 9-borafluorenes, direct chemical reduction of **1a** or **1b** proved experimentally challenging and did not meet with success in providing useful reagents for metathesis with appropriate metal chlorides.[12] To explore the coordination chemistry of compounds **1**, we thus chose an approach used principally by Herberich et al. for preparing borollide complex, which involves reaction of neutral compounds **1** with an appropriate low-valent organometallic fragment.[3a] In this process, the interaction of the electron-rich metal center with the empty $2p_z$ orbital localized on boron induces the spontaneous aromatization of the borole ring with the simultaneous oxidation of the metal.[13]

The low-valent main group metallocene $[Cp^*Al]_4$ ($Cp^* = \eta^5$-$C_5Me_5$) originally reported by Schnöckel and co-workers[14] behaves as a Lewis base toward $B(C_6F_5)_3$, leading to the formation of $Cp^*Al{\cdot}B(C_6F_5)_3$.[15] Given the tendency of Cp*Al(I) to form Al(III) derivatives,[16] we surmised that in reaction with 9-borafluorenes **1**, such an $\eta^1$ adduct might convert to an $\eta^5$ compound isoelectronic with the aluminocenium cation.[17] As described herein, this expectation proved erroneous, not only for the fluorinated 9-borafluorenes **1**, but also for the related nonfluorinated species $C_{12}H_8B(C_6H_5)$, **2**.

**Scheme 1**

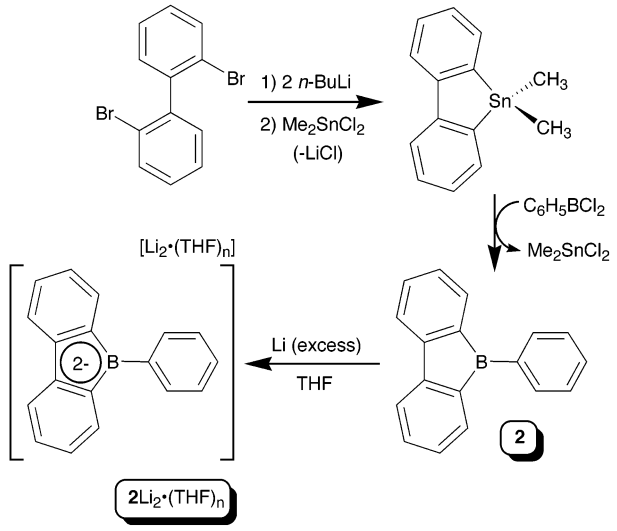


## Results and Discussion

**Synthesis of 9-Borafluorenes.** The syntheses of the fluorinated compounds **1** were carried out as described previously.[11] The original procedure for preparing the nonfluorinated counterpart of **1a**, 9-phenyl-9-borafluorene **2**, involved the high-temperature thermolysis of a diphenyl-2-biphenyl borane and gave only moderate yields of **2**. Thus, we adapted the synthetic route used to prepare **1a** to accommodate **2** as shown in Scheme 1. Addition of 2 equiv of *n*-BuLi to $C_{12}H_8Br_2$ and subsequent quenching with $Me_2SnCl_2$ afforded, after removal of the solvent, pure $C_{12}H_8SnMe_2$ in virtually quantitative yield (98%). The $^1$H NMR spectrum of this compound showed an upfield singlet signal for the Sn-Me groups centered at $\delta$ 0.27 ppm with the diagnostic $^{117}$Sn/$^{119}$Sn satellites ($^2J_{Sn-H}$ = 57.8 Hz, 60.2 Hz). The aromatic zone was composed of complex multiplets assigned to the hydrogen atoms of the biphenyl framework, which gave satisfactory integration. The $^{119}$Sn{$^1$H} NMR spectrum showed a singlet at $\delta$ −34.1 ppm.

The stannole $C_{12}H_8SnMe_2$ reacted with $C_6H_5BCl_2$ at −78 °C in toluene, generating a bright yellow solution containing **2** and $Me_2SnCl_2$ as the sole products as judged by NMR spectroscopy. Removal of $Me_2SnCl_2$ by sublimation gave **2**, which was obtained in almost quantitative yield. Analytical and spectral data for this compound were as expected, and the $^{11}$B{$^1$H} NMR spectrum gave a single broad signal centered at $\delta$ 64.5 ppm.

Although dianionic derivatives of fluorinated 9-borafluorenes **1** are not accessible via direct chemical reduction from their neutral precursors, the less Lewis acidic **2** is smoothly reduced in THF solution, using an excess of lithium powder (Scheme 1). After filtering off the excess Li and removing the THF, the product was extracted into toluene and precipitated using pentane. 9-Boratafluorene **2**$Li_2{\cdot}(THF)_n$ is isolated as THF solvate with a variable number of molecules depending on the experimental conditions. The $^{11}$B{$^1$H} NMR of **2**$Li_2{\cdot}(THF)_n$ showed a sharp signal at $\delta$ 6.2 ppm, which is in

(7) Koster, R.; Benedikt, G. *Angew. Chem., Int. Ed. Engl.* **1963**, *2*, 323.
(8) Eisch, J. J.; Galle, J. E.; Kozima, S. *J. Am. Chem. Soc.* **1986**, *108*, 379.
(9) Grigsby, W. J.; Power, P. P. *J. Am. Chem. Soc.* **1996**, *118*, 7981.
(10) (a) Wehmschulte, R. J.; Khan, M. A.; Twamley, B.; Schiemenz, B. *Organometallics* **2001**, *20*, 844. (b) Wehmschulte, R. J.; Diaz, A. A.; Khan, M. A. *Organometallics* **2003**, *22*, 83.
(11) Chase, P. A.; Piers, W. E.; Patrick B. O. *J. Am. Chem. Soc.* **2000**, *122*, 12911.
(12) (a) Romero, P.; Chase, P. A.; Piers, W. E.; Parvez, M. Manuscript in preparation. Similar observations in the reduction of $B(C_6F_5)_3$ vs $B(C_6H_5)_3$ have been encountered: (b) Harlan, C. J.; Hascall, T.; Fujita, E. Norton, J. R. *J. Am. Chem. Soc.* **1999**, *121*, 7274. (c) Kwaan, R. J.; Harlan, J.; Norton, J. R. *Organometallics* **2001**, *20*, 3818.
(13) Formation of stable diene-like complexes has been observed, for instance, in systems where conjugation between the exocyclic substituent and boron exists. See for example: Herberich, G. E.; Hessner, B.; Ohst, H.; Raap, I. A. *J. Organomet. Chem.* **1988**, *348*, 305.
(14) (a) Dohmeier, C.; Robl, C.; Schnöckel, H. *Angew. Chem., Int. Ed. Engl.* **1991**, *30*, 564. (b) Dohmeier, C.; Loos, D.; Schnöckel, H. *Angew. Chem., Int. Ed. Engl.* **1996**, *35*, 129. (c) Schulz, S.; Roesky, H. W.; Kocj, H J.; Sheldrick, G. M.; Stalke, D.; Kuhn, A. *Angew. Chem., Int. Ed. Engl.* **1993**, *32*, 1729.
(15) Gorden, J. D.; Voigt, A.; Macdonald, C. L. B.; Silverman, J. S.; Cowley, A. H. *J. Am. Chem. Soc.* **2000**, *122*, 950.
(16) (a) Rao, M. N. S.; Roesky, H. W.; Anantharaman, G. *J. Organomet. Chem.* **2002**, *646*, 4. (b) Himmel, H.-G.; Vollet, J. *Organometallics* **2002**, *21*, 5972.
(17) Dohmeier, C.; Schnöckel, H.; Robl, C.; Schneider, U.; Ahlrichs, R. *Angew. Chem., Int. Ed. Engl.* **1993**, *32*, 1655.

accord with values reported for related compounds.[9,10] The symmetry of the signals in the aromatic region observed in the $^1$H NMR spectrum of **2**$Li_2$·$(THF)_n$ resembled the pattern reported for the related 9-phenyl-9-borataanthracene.[18]

**Reactions of 9-Borafluorenes with [Cp*Al]$_4$.** The reaction between $[Cp^*Al]_4$ and **1a** took place instantaneously in toluene solution as judged by the change in color of the solutions from bright yellow to orange (eq 1). $^1$H NMR analysis showed that the signal for the

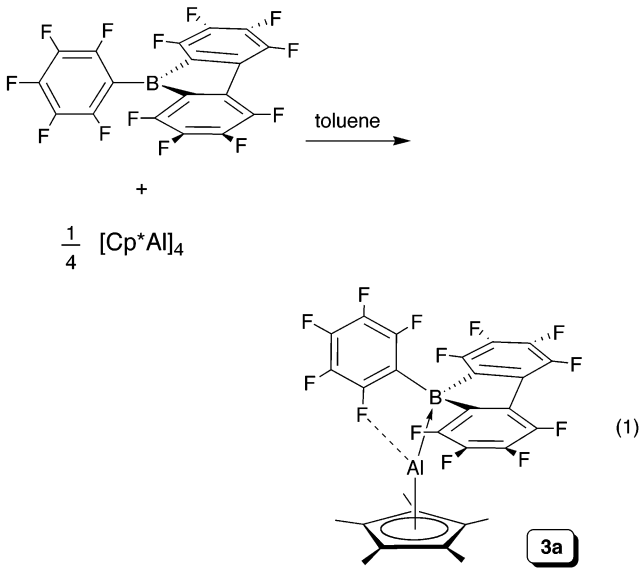


(1)

protons of the Cp* shifted upfield from $\delta$ 1.90 ppm to $\delta$ 1.11 ppm upon formation of product **3a**, while the $^{19}$F NMR spectrum showed seven new signals. Inspection of the resonances due to the $-C_6F_5$ ring indicated the difference between *meta*- and *para*-fluorine shifts of $\Delta\delta_{m,p} = 5.6$ ppm.[19] The $^{11}$B{$^1$H} NMR spectrum showed a single resonance at $\delta$ −25.4 ppm. These data compare favorably with that found for $Cp^*Al{\cdot}B(C_6F_5)_3$ ($\Delta\delta_{m,p}$ = 4.9 ppm; $^{11}$B{$^1$H} $\delta$ −32.9 ppm [15]) and is thus consistent with the formation of an $\eta^1$ Lewis acid−base adduct. $^{27}$Al NMR measurements, however, were ambiguous. Product **3a** exhibits an extremely upfield resonance at $\delta$ −114.3 ppm that could indicate the presence of an Al(I) center, but is also consistent with an $\eta^5$ structure, since the $[Cp^*_2Al]^+$ cation resonates in this region of the spectrum as well ($\delta$ −114.5 ppm). The upfield shift for $[Cp^*_2Al]^+$ has been rationalized in terms of a diamagnetic ring current effect of the Cp* ligands.[17]

To fully characterize the bonding mode in **3a**, a single-crystal X-ray diffraction study was carried out. Yellow crystals of the product **3a** could be isolated by mixing the reactants in toluene solution and layering with hexanes at −35 °C. This experiment confirmed that **3a** is an $\eta^1$ Lewis acid−base adduct; a thermal ellipsoid diagram and selected metrical parameters are provided

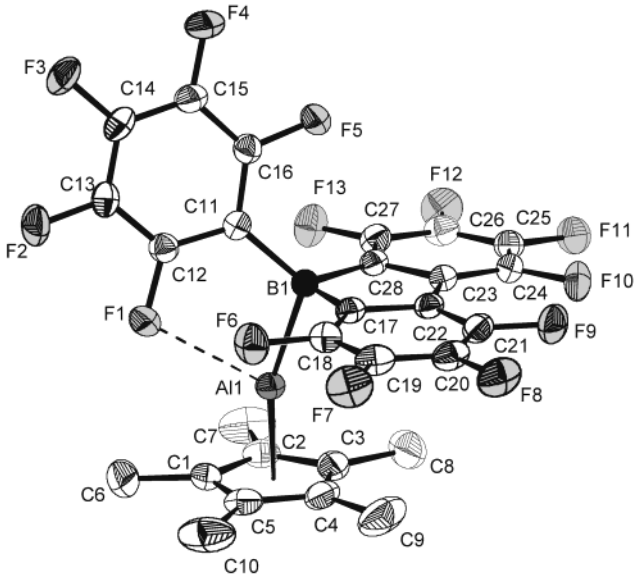


**Figure 1.** Molecular structure of **3a**. Selected bond distances (Å): B(1)−Al(1), 2.1147(15); Al(1)−Cp*(average), 2.1560(32); B(1)−C(11), 1.6137(19); B(1)−C(28), 1.6038(19); B(1)−C(17), 1.6054(19); C(28)−C(23), 1.4228(18); C(17)−C(22), 1.4213(18); C(12)−F(1), 1.3611(16); Al(1)−F(1), 2.800; C(16)−F(5), 1.3461(15). Selected bond angles (deg): B(1)−Al(1)−Cp*(centroid), 160.95; Al(1)−B(1)−C(11), 113.64(9); C(11)−C(12)−F(1), 120.12(12); C(11)−C(16)−F(5), 119.76(11).

in Figure 1. The Cp* group is bonded in a $\eta^5$ fashion to aluminum, and the average Al(1)−Cp* distance of 2.1560(32) Å compares well with those of $Cp^*Al{\cdot}B(C_6F_5)_3$ (2.171(5) Å) or $[Cp^*_2Al]^+$ (2.155 Å),[17] but it is considerably shorter than that found in tetrameric $[Cp^*Al]_4$ (2.344 Å)[14a] or in monomeric Cp*Al (2.388(7) Å) (determined by gas-phase electron diffraction).[20] The distance Al(1)−B(1) (2.1147(15) Å), however, is shorter when compared to $Cp^*Al{\cdot}B(C_6F_5)_3$ by about 0.05 Å.

The angle B(1)−Al(1)−Cp*(centroid) of 160.95° contrasts with the virtually linear angle found for $Cp^*Al{\cdot}B(C_6F_5)_3$ (172.9°). Apparently the bending allows for a stabilizing dative interaction between an *ortho*-fluorine atom and the Lewis acidic aluminum center (Al(1)−F(1) = 2.800(13) Å). Although direct comparative data are absent from the literature, values of between 2.414(3) and 2.267(5) Å for related dative C−F→Zr interactions[21] and contacts in the range of 2.54−2.72 Å for C−F→In(I) bonds[22] suggest that the donation in **3a** is quite weak. Nonetheless, variable-temperature $^{19}$F NMR experiments performed on **3a** in $CD_2Cl_2$ solution revealed restricted rotation around the B−C bond on the $-C_6F_5$ substituent. At room temperature, a broad signal was observed at $\delta$ −129.8 ppm corresponding to the *ortho*-fluorines of the $-C_6F_5$ ring, which split into two resonances at −125.9 and −132.5 ppm upon cooling to 200 K. Similar behavior was observed in the *meta*-fluorine resonances. Analysis of the spectra yields a $\Delta G^{\ddagger}_{rotation}$ of 42.2(5) kJ mol$^{-1}$ at a coalescence temperature of 243 K. This spectral behavior is possibly

(18) Lee, R. A.; Lachicotte, R. J.; Bazan, G. C. *J. Am. Chem. Soc.* **1998**, *120*, 6037.

(19) The charge and coordination environment of a boron atom attached to a pentafluorophenyl ring ($C_6F_5$) is found to correlate directly with the chemical shift difference between the *para*- and *meta*-fluorine ($\Delta\delta_{m,p}$) in the $^{19}$F NMR spectrum, which is a particularly useful tool for reactions with $B(C_6F_5)_3$. See: Horton, A. D.; de With, J. *Organometallics* **1997**, *16*, 5424. We have found that **1a**, which possesses a $-C_6F_5$ substituent, behaves similarly.

(20) Haaland, A.; Martinsen, K.; Shlykov, S. A.; Volden, H. V.; Dohmeier, C.; Schnöckel, H. *Organometallics* **1995**, *14*, 3116.

(21) Sun, Y.; Spence, R. E. v. H.; Piers, W. E.; Parvez, M.; Yap, G. P. A. *J. Am. Chem. Soc.* **1997**, *119*, 5132.

(22) Wright, R. J.; Phillips, A. D.; Hardman, N. J.; Power, P. P. *J. Am. Chem. Soc.* **2002**, *124*, 8538.

indicative of a low-energy solution structure akin to that seen in the solid state.

Adduct **3a** is highly thermally stable. Heating samples to 110 °C for 2 days resulted in little change in either the $^1$H or $^{19}$F NMR spectra, negating the possibility of a kinetic barrier between the $\eta^1/\eta^5$ bonding modes. Furthermore, no substantial change was observed when the solution was monitored by high-temperature NMR spectroscopy. Rationalizing that the preference of an $\eta^1$ over an $\eta^5$ bonding mode in **3a** might be due to unfavorable steric interactions between the Cp* ring and the $C_6F_5$ ring lying nearly orthogonal to the borafluorene plane,[23] we carried out the reaction of $[Cp^*Al]_4$ with **1b**. In addition to being less sterically significant, the methyl substituent should result in a less Lewis acidic boron center.

Reaction between $[Cp^*Al]_4$ and perfluorinated 9-methyl-9-borafluorene **1b** in bromobenzene afforded complex **3b** in moderate yields (eq 2). Crystals could be obtained

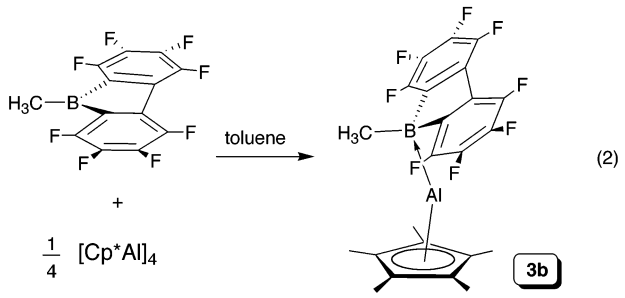


(2)

by cooling the solution at −35 °C overnight. The spectroscopic features exhibited by **3b** were similar to those of $\eta^1$ adduct **3a**, and X-ray analysis confirmed a similar bonding arrangement in **3b**. A thermal ellipsoid diagram and pertinent metrical parameters are provided in Figure 2. The solid structure of **3b** consists of an array of two independent molecules in the unit cell, which differ in that one of the adducts shows an intermolecular interaction through C−H···F hydrogen bonds (Figure 2b). The F−C distance of 3.208 Å is shorter than those reported by Desiraju for a series of fluorobenzene derivatives.[24] Intramolecular metrical parameters for the two molecules are almost identical, and key data compare well with that found for the adduct **3a**. This is the case even for the B(1)−Al(1)−Cp*(centroid) angle, which is 162.76° in **3b**. In this instance, the bend is likely a consequence of packing forces, since the orientation of the Cp*Al fragment with respect to the Lewis acid is different from that seen in **3a**. The boron center shows a distorted tetrahedron environment with an angle C(2)−B(1)−C(13) of 98.7(5)°, which is virtually identical to that reported for the ion pair $Cp_2ZrMe(\mu\text{-Me})Me\text{-}B(C_{12}F_8)$ (97.2(2)°).[11]

Attempts to thermally convert $\eta^1$-**3b** to an $\eta^5$ structure were similarly unfruitful, indicating that even for the less sterically bulky borafluorene **1b**, the $\eta^1$ structure is thermodynamically favored. In a final attempt to produce an $\eta^5$ aluminocenium analogue, the reaction of

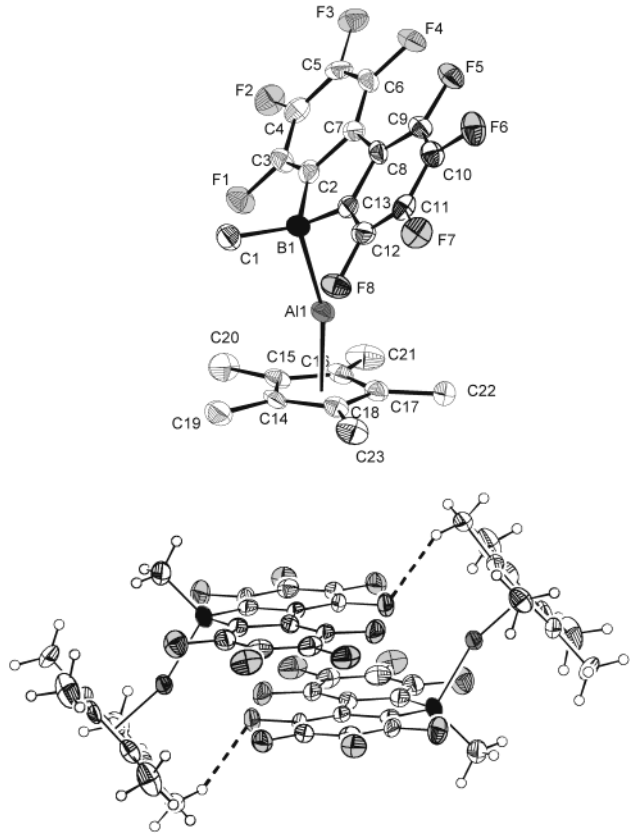


**Figure 2.** Molecular structure of **3b** showing the two different arrangements found in the unit cell. Selected bond distances (Å): B(1)−Al(1), 2.149(7); Al(1)−Cp*(average), 2.185(13); B(1)−C(1), 1.634(9); B(1)−C(2), 1.602(9); B(1)−C(13), 1.614(9). Selected bond angles (deg): B(1)−Al(1)−Cp*(centroid), 162.76; Al(1)−B(1)−C(1), 103.4(4); C(2)−B(1)−C(13), 98.7(5); C(2)−B(1)−C(1), 117.3(5).

$[Cp^*Al]_4$ with the nonfluorinated 9-phenyl-9-borafluorene **2** was explored, the idea being that a less Lewis acidic boron center might disfavor the $\eta^1$ bonding mode. The reaction of **2** and $[Cp^*Al]_4$ was not as clean as the previously described reactions, as precipitation of colloidal aluminum metal accompanied product formation. After heating the mixture for a short period of time, the aluminum metal was separated by filtration and yellow crystals of a new compound, **4**, were obtained from the filtrate in moderate yields (eq 3). Microanalysis of

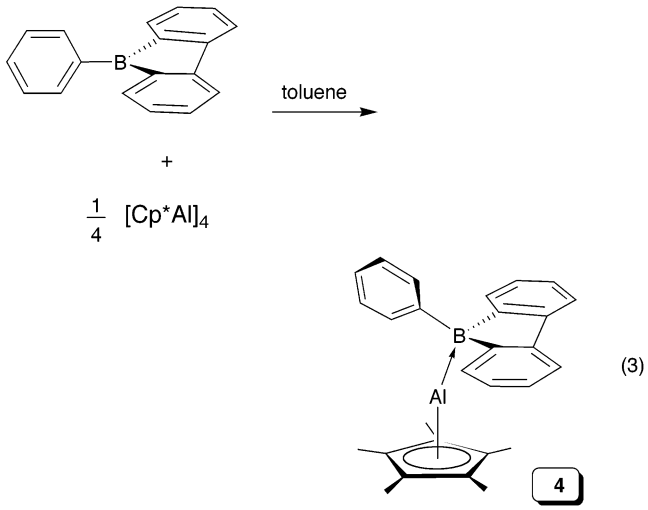


(3)

(23) Cowley et al. have demonstrated that in the case of decamethylborocenium cation, $[Cp^*_2B]^+$, the observed $\eta^1(\sigma)/\eta^5(\pi)$ arrangement can be explained in part by steric congestion: Voigt, A.; Filliponi, S.; Macdonald, C. L. B.; Gorden, J. D.; Cowley, A. H. *Chem. Commun.* **2000**, 911.

(24) Thalladi, V. R.; Weiss, H.-C.; Blaser, D.; Boese, R.; Nangia, A.; Desiraju, G. R. *J. Am. Chem. Soc.* **1998**, *120*, 8702.

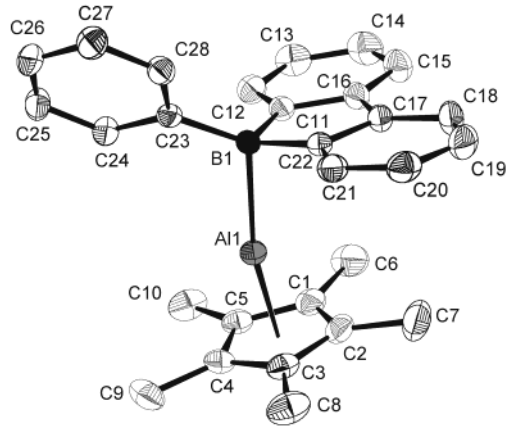


**Figure 3.** Molecular structure of **4**. Selected bond distances (Å): B(1)−Al(1), 2.1347(13); Al(1)−Cp*(average), 2.1792; B(1)−C(23), 1.5963(16); B(1)−C(11), 1.6133(17); B(1)−C(22), 1.6091(17). Selected bond angles (deg): B(1)−Al(1)−Cp*(centroid), 164.12; Al(1)−B(1)−C(23), 114.92(8); C(11)−B(1)−C(22), 110.19(9); C(11)−B(1)−C(23), 119.46(10); C(22)−B(1)−C(23), 123.86(10).

the crystals confirmed a 1:1 ratio between the Cp*Al and **2**. The $^1$H NMR spectrum showed a singlet at $\delta$ 1.19 ppm and the expected signals in the aromatic region. Sharp signals in the $^1$H NMR spectrum were dependent on the absence of even traces of $[Cp^*Al]_4$ reagent; when added to samples of **4**, the resonance for the Cp* protons broadened considerably, suggesting that exchange between bound and free Cp*Al is facile in this system. This contrasts with the nonlability of the Lewis base in adducts **3**, but perhaps explains why precipitation of colloidal Al is observed in this case. It has been observed, for example, that biasing the tetramer/monomer equilibrium present in solutions of $[Cp^*Al]_4$ toward the monomer, either by heat or by addition of a Lewis acid such as $AlCl_3$,[25] leads to substantial deposition of aluminum. Furthermore, **4** is much less thermally stable in solution than its fluorinated counterparts, slowly decomposing at room temperature over a period of days, to yield aluminum metal as the main observable byproduct, along with Cp*H and some unidentified organometallic Al(III) species. These observations are more consistent with an $\eta^1$ bonding mode for **4**; the $^{11}$B{$^1$H} NMR ($\delta$ −4.9 ppm) and $^{27}$Al NMR ($\delta$ −70.3 ppm) spectra are also indicative of such a structure, which was again confirmed crystallograpically.

A thermal ellipsoid diagram of $\eta^1$-**4** along with selected metrical parameters are provided in Figure 3. There are no unusually short contacts in the crystal structure, and, as in the previous examples, the Cp* ring is bonded in a $\eta^5$ mode to the aluminum center. The angle B(1)−Al(1)−Cp*(centroid) of 164.12° is in the same range as those observed for **3a**,**b**, while the distance B(1)−Al(1) of 2.1347(13) Å is also very close to the distances observed for the other adducts. The boron center in **4** shows a distorted tetrahedral environment with an angle C(11)−B(1)−C(22) of 110.19(9)°, which is about 11° wider compared with the same angles in **3a**,**b**.

**Scheme 2**

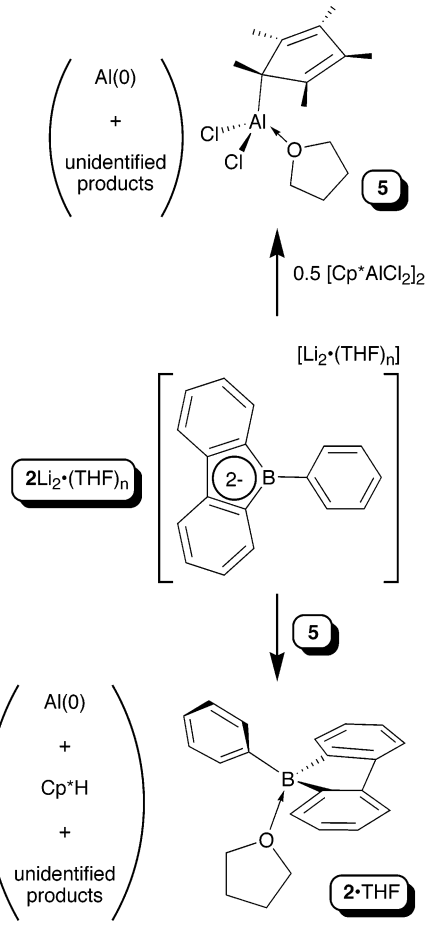


**Reaction of $2Li_2$·$(THF)_n$ with $Cp^*AlCl_2$(THF).** The availability of the dilithium salt of **2** suggested an alternative route to the putative $\eta^5$ 9-boratafluorene aluminum compound via metathesis with $[Cp^*AlCl_2]_2$,[26] which is the starting material for the synthesis of $[Cp^*Al]_4$. Since reaction of $\mathbf{2}Li_2$·$(THF)_n$ and $[Cp^*AlCl_2]_2$ leads initially to the THF-stabilized complex $Cp^*AlCl_2$·(THF), **5**, via transfer of a THF molecule from lithium to aluminum, we prepared **5** separately for use in subsequent reactions (Scheme 2). The identity of **5** was confirmed by X-ray analysis. A thermal ellipsoid diagram is provided in Figure 4. The solid structure confirmed the presence of a coordinated molecule of THF with an Al(1)−O(1) distance of 1.8332(15) Å. This distance is slightly shorter than the range of 1.852(1)−1.902(5) Å found for other $RAlCl_2$·THF adducts.[27] The compound features an $\eta^1$ $\sigma$-bonded Cp* ligand with a distance between Al(1) and the cyclopentadienyl carbon C(1) of 2.009(2) Å, within the range observed for other $\eta^1$-bonded cyclopentadienyl derivatives of aluminum.[28] In solution, the presence of a singlet for the Cp* methyls in the $^1$H NMR spectrum even at 200 K is consistent

(25) Gauss, J.; Schneider, U.; Ahlrichs, R.; Dohmeier, C.; Schnöckel, H. *J. Am. Chem. Soc.* **1993**, *115*, 2402.

(26) Koch, H.; Schulz, S.; Roesky, H. W.; Noltemeyer, M.; Schmidt, H.; Heine, A.; Herbst-Irmer, R.; Stalke, D.; Sheldrick, G. M. *Chem. Ber.* **1992**, *125*, 1107.

(27) (a) Petrie, M. A.; Power, P. P.; Rasika Dias, H. V.; Ruhlandt-Senge, K.; Waggoner, K. M.; Wehmschulte, R. J. *Organometallics* **1993**, *12*, 1086. (b) Wehmschulte, R. J.; Power, P. P. *Inorg. Chem.* **1996**, *35*, 3262. (c) Schnitter, C.; Klimek, K.; Roesky, H. W.; Albers, T.; Schmidt, H.-G.; Röpken, C.; Parisini, E. *Organometallics* **1998**, *17*, 2249. (d) Eaborn, C.; Hitchcock, P. B.; Smith, J. D.; Sözerli, S. E. *Organometallics* **1998**, *17*, 4322.

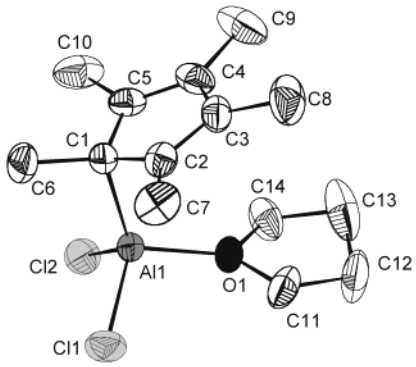


**Figure 4.** Molecular structure of **5**. Selected bond distances (Å): Al(1)−C(1), 2.009(2); Al(1)−Cl(1), 2.1392(8); Al(1)−Cl(2), 2.1439(9); Al(1)−O(1), 1.8332(15); C(1)−C(6), 1.530(3); C(1)−C(2), 1.475(3); C(1)−C(5), 1.467(3); C(2)−C(3), 1.370(3); C(5)−C(4), 1.355(3); C(3)−C(4), 1.445(3). Selected bond angles (deg): C(1)−Al(1)−O(1), 113.81(8); Cl(1)−Al(1)−Cl(2), 106.91(4); Cl(1)−Al(1)−O(1), 103.79(6); Cl(1)−Al(1)−C(1), 111.99(7); C(1)−Al(1)−Cl(2), 116.77(7); Cl(2)−Al(1)−O(1), 102.33(6); Al(1)−C(1)−C(6), 109.34(15); C(2)−C(1)−C(5), 104.77(17).

with a highly fluxional structure, which is a common feature of cyclopentadienyl derivatives of aluminum.[28]

The reaction of **2**$Li_2$·$(THF)_n$ and **5** was carried out at −78 °C in THF and slowly warmed to room temperature, during which time the dark red-brown color corresponding to **2**$Li_2$·$(THF)_n$ disappeared and an intense blue color was observed at about 0 °C. Once the reaction reached room temperature, the blue color disappeared and a pale yellow solution was obtained along with a deposit of colloidal aluminum metal. Analysis of the solid obtained after filtration and removal of the solvent indicated the presence of Cp*-H and the THF adduct of the neutral 9-phenyl-9-borafluorene, **2**·(THF), as the main identifiable products (Scheme 2). The latter was positively identified by treating **2** with a stoichiometric amount of THF.

It thus seems that, even by this metathesis route, the $\eta^5$-boratafluorene structure is not accessible. Rather, the dilithio salt of **2** functions as a reducing agent, a notion supported by the observation of the transient deep blue color, which is suggestive of a boron-based radical anion[12c,29] Our results are also in accord with those of Wehmschulte,[10] who observed reduction behavior when sterically encumbered 9-boratafluorenes were reacted with metal halides. These compounds thus exhibit a strong tendency toward $\eta^1$ adducts when bonding to the Cp*Al fragment. To understand this phenomenon in more detail, DFT computations were undertaken.

**Computational Studies.** DFT computations at the B3LYP/6-31G** level were performed on CpAl and Cp*Al adducts of the parent borole ($C_4H_5B$) and 9-borafluorene ($C_{12}H_9B$) Lewis acids (Chart 2). Geometry optimizations were initiated from both $\eta^1$ and $\eta^5$ structures, and it was found that the borole minimized to $\eta^5$ structures, while the 9-borafluorene minimized to $\eta^1$ adducts. By imposing a number of geometric constraints, it was possible to partially optimized the structures of $\eta^1$-**I**-AlCp and $\eta^5$-**II**-AlCp, thereby providing an estimate, albeit an upper limit, of the energy difference between these complexes and the preferred coordination complexes of **I**-AlCp and **II**-AlCp, which was predicted to be 13.2 and 18.6 kcal/mol, respectively. Selected metrical parameters for the four optimized structures, along with experimental data from **4**, are shown in Table 1. Overall, the agreement between the experimental data and the calculated values for the $\eta^1$-borafluorene adducts is quite good. It should be added that the same coordination preferences were predicted for complexes of AlCp with **I** and **II** when the H substituent on the B atom was replaced with bulkier $CH_3$ and phenyl groups.

**Table 1. Summary of Optimized Geometric Parameters**

| parameter | **I**-CpAl | **I**-Cp*Al | **II**-CpAl | **II**-Cp*Al | **4** |
|---|---|---|---|---|---|
| Al−B | 2.165 | 2.177 | 2.210 | 2.180 | 2.135 |
| Al−$C_\alpha$ | 2.104 | 2.114 | 2.850 | 2.890 | 2.819 |
| Al−$C_\beta$ | 2.216 | 2.223 | 3.535 | 3.623 | 3.510 |
| Al−$C_{Cp}$ | 2.294 | 2.253 | 2.286 | 2.251 | 2.180 |
| B−$C_\alpha$ | 1.553 | 1.550 | 1.602 | 1.605 | 1.611 |
| $C_\alpha$−$C_\beta$ | 1.451 | 1.451 | 1.424 | 1.424 | 1.419 |
| $C_\beta$-$C_{\beta'}$ | 1.415 | 1.414 | 1.475 | 1.474 | 1.468 |
| H−B−Al | 124 | 123 | 109 | 109 | 115 |
| H−B−$C_\alpha$ | 129 | 129 | 124 | 123 | 120 |
| H−B−$C_\alpha$−$C_\beta$ | 1 | 1 | 34 | 39 | 41 |

**Chart 2**

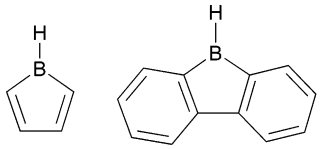


**I** **II**

Examination of the $\pi$-symmetric molecular orbitals of the borole and 9-borafluorene rings provides insight as to why the latter strongly prefers $\eta^1$ coordination. The $\pi$ orbitals of **I** used to bond with the CpAl fragment orbitals are Cp-like, with two nondegenerate $\pi$-symmetric orbitals due to the broken symmetry of the boracyclic ring. In **II**, however, the $\pi$ orbitals of the flanking phenyl rings mix with the $\pi$ orbitals of the central borole ring, through both in-phase and out-of-phase combinations. In-phase mixing lowers the energy of the MO with respect to that in **I**, while out-of-phase mixing results in a slight increase in the orbital energy. The MO correlation diagram displayed in Figure 5 illustrates how the $\pi$-symmetric MOs of the 9-borafluoorene ring arise from those of the parent borole ring via conjugation onto the phenyl rings. As evident in Figure 5, the aromaticity in the 9-borafluorene system is localized in the phenyl rings, leaving the LUMO largely associated with the boron center.

To gain further insight into the preferred bonding modes of these compounds, the fragment orbital analysis scheme of Ziegler and Rauk[30] was employed to examine the nature of the interaction between CpAl and the borole and 9-borafluorene rings in **I**-CpAl and **II**-CpAl. In this approach the MOs of a complex AB (**I**-AlCp or **II**-AlCp) are reconstructed in terms of the MOs

(28) (a) Shapiro, P. J. *Coord. Chem. Rev.* **1999**, *189*, 1. (b) Fisher, J. D.; Budzelaar, P. H. M.; Shapiro, P. J.; Staples, R. J.; Yap, G. P. A.; Rheingold, A. L. *Organometallics* **1997**, *16*, 871. (c) Pietryga, J. M.; Gorden, J. D.; Macdonald, C. L. B.; Voigt, A.; Wiacek, R. J.; Cowley, A. H. *J. Am. Chem. Soc.* **2001**, *123*, 7713.

(29) For example, the radical anion of $BPh_3$ is reported to be blue in color: (a) Dupont, T. J.; Mills, J. L. *J. Am. Chem. Soc.* **1975**, *97*, 6375. (b) Schulz, A.; Kaim, W. *Chem. Ber.* **1989**, *122*, 1863.

(30) Ziegler, T.; Rauk, A. *Theor. Chim. Acta* **1977**, *49*, 143.

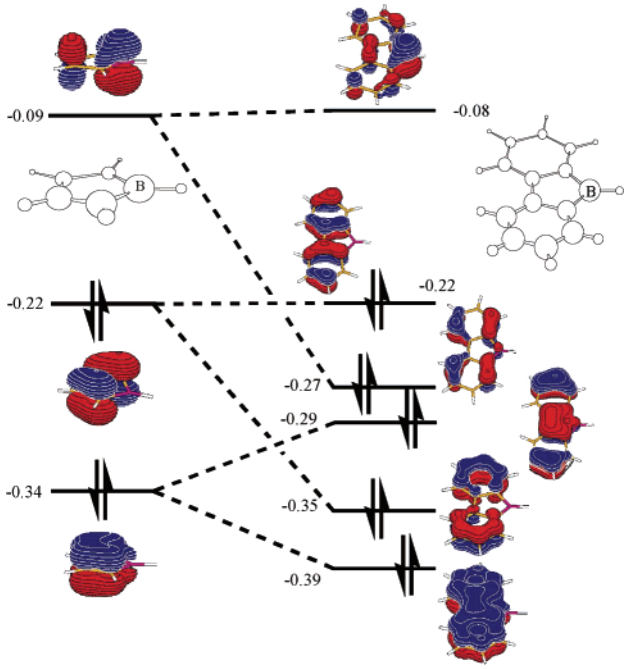


**Figure 5.** MO correlation diagram to illustrate how the $\pi$-symmetric MOs of the parent borole ring change due to conjugation onto the phenyl rings in the 9-borafluorene ring. (Pictorial representations of the molecular structures are also provided to give the reader a frame of reference to interpret the MOs.)

of its constituent fragements A (**I** or **II**) and B (AlCp). The bonding in **I**-CpAl is akin to that expected for a metallocenium cation. Of particular interest is the interaction between the CpAl HOMO and the borole LUMO, which is positive due to the greater emphasis of the latter orbital on $C_\alpha-B-C_{\alpha'}$; however, the overlap is only 0.17 (Figure 6a). In **II**-CpAl the most significant bonding interaction also involves mixing of the 9-borafluorene LUMO with the CpAl HOMO (Figure 6b). In this case, since the 9-borafluorene LUMO is largely associated with the boron atom, the overlap for this interaction is significantly larger than the analogous overlap for the borole ring (0.33 vs 0.17). Furthermore, in **II**-AlCp the Al→B interaction is bolstered by the interaction of the CpAl HOMO with the 9-borafluorene HOMO-2 (Figure 6c), which arises via in-phase mixing of the borole LUMO with the $\pi$ orbitals of the flanking phenyl rings (see Figure 5). Although, the overlap in this second bonding orbital is smaller at 0.18, the interaction does stablize the $\eta^1$ bonding mode for the 9-borafluorene complexes. This interaction is not possible in the parent borole, thereby leading to its preference for the $\eta^5$ coordination geometry when bound to AlCp.

## Conclusions

In summary, in an attempt to explore the coordination chemistry of a series of 9-borafluorenes, we have found a strong thermodynamic preference for $\eta^1$ bonding modes with the Lewis base Cp*Al(I). Given the propensity of Al(I) to be oxidized to Al(III), and the perceived legitimacy of an ($\eta^5$-9-borafluorene)AlCp* product, the stability of the $\eta^1$ adducts was something of a surprise. While aromatization of the borole ring via the addition

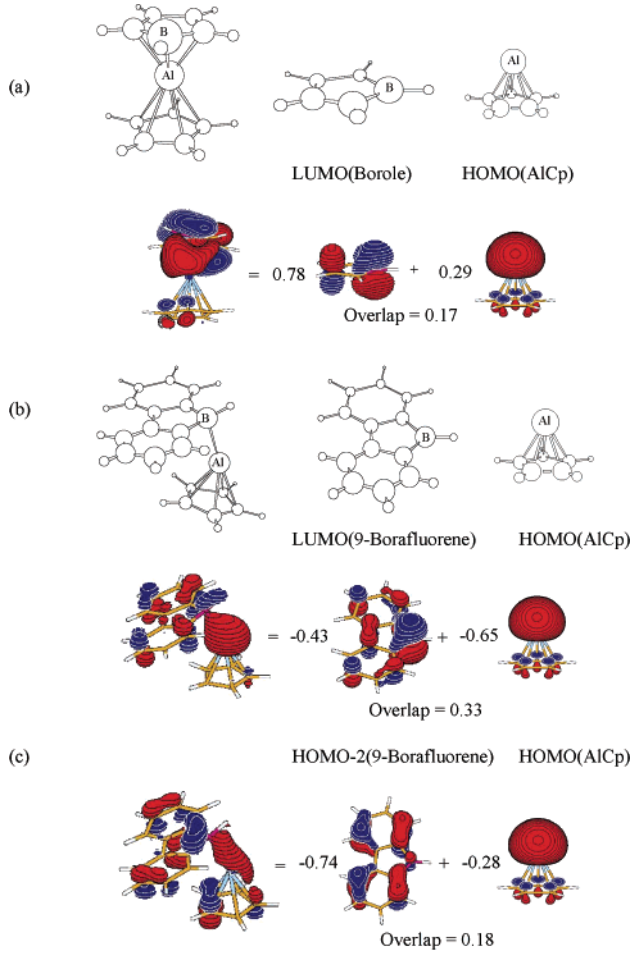


**Figure 6.** Summary of the fragment orbital analyses of the important MO interactions in **I**-AlCp and **II**-AlCp. The MOs of the complex and the corresponding constituent fragment orbitals are displayed, along with their respective coefficients and the overlap between them. (Pictorial representations of the molecular structures are also provided to give the reader a frame of reference to interpret the MOs.)

of two electrons and formation of an $\eta^5$ structure is favorable for the parent system, this process is disfavored in the 9-borafluorenes because aromatization of the five-membered borole core comes at the expense of the aromatic character of the phenyl rings. Thus, the Cp*Al fragment functions only as a Lewis base electron pair donor rather than a formal two-electron reducing agent and forms $\eta^1$ structures exclusively with 9-borafluorenes. The implications of these observations for the prospects of 9-borafluorenes serving as $\eta^5$ donors for transition metals are not clear, but the fact that dilithio salts of 9-borafluorenes exhibit structural parameters consistent with an aromatized $C_4B$ ring[9,10] suggests that $\eta^5$ bonding modes should be possible for highly reducing metals.

## Experimental Section

**General Procedures.** Argon-filled Innovative Technology System One dryboxes were used to store air- and moisture-sensitive compounds and for manipulation of air-sensitive materials. Reactions were performed either on a double-manifold vacuum line using standard Schlenk techniques or under an argon atmosphere in the drybox for small-scale

reactions. $C_6H_5BCl_2$, $Me_2SnCl_2$, $C_6H_4Br_2$, $C_5Me_5$-H, and Li powder (0.5% Na) were purchased from Aldrich and used without further purification. $AlCl_3$ (99%) was also purchased from Aldrich and additionally purified by sublimation under full dynamic vacuum at 140 °C. **1a**,**b**,[11] $C_{12}H_8Br_2$,[31] Cp*$AlCl_2$,[26] and [Cp*Al]$_4$[14c] were prepared according to known literature procedures. Toluene, hexanes, and tetrahydrofuran (THF) were purified using the Grubbs/Dow system[32] and stored in glass bombs over an appropriate indicator (titanocene for toluene and hexanes, sodium/benzophenone ketyl for THF). Diethyl ether ($Et_2O$) was predried over calcium hydride overnight and then distilled and stored over sodium/benzophenone ketyl in a glass bomb. All deuterated solvents were purchased from Cambridge Isotopes. $C_7D_8$ and $C_6D_6$ were distilled from sodium/benzophenone ketyl and stored in appropriate glass bombs. $d_8$-THF was also distilled from sodium/benzophenone and stored over 4 Å molecular sieves. $CD_2Cl_2$ was distilled from $CaH_2$. Where applicable, liquid reagents were degassed by repeated freeze−pump−thaw cycles. Nuclear magnetic resonance (NMR) spectra were obtained on Bruker ACE-200 ($^1$H, 200.134 MHz), AMX 300 ($^1$H 300.138 MHz, $^{19}$F 282.371 MHz), and BAM-400 ($^1$H 400.134 MHz, $^{13}$C 100.614 MHz, $^{11}$B 128.377 MHz, $^{119}$Sn 149.211 MHz, $^{27}$Al 104.264 MHz). All $^1$H and $^{13}$C spectra were referenced externally to $Me_4Si$ at 0 ppm by referencing the residual solvent peak. $^{11}$B NMR, $^{119}$Sn NMR, and $^{27}$Al NMR spectra were referenced externally relative to $BF_3{\cdot}Et_2O$, $Me_4Sn$, and $Al(H_2O)_6^{3+}$ at 0 ppm, respectively. $^{19}$F NMR were referenced externally to $C_6F_6$ at −163 ppm relative to $CFCl_3$ at 0 ppm. Elemental analyses were performed by Dorothy Fox or Roxanna Simank using a Control Equipment Corporation 440 elemental analyzer.

**Synthesis of $C_{12}H_8SnMe_2$.** $C_{12}H_8Br_2$ was placed in a 100 mL round-bottom flask (1.0 g, 3.2 mmol), and diethyl ether (60 mL) was condensed onto the solid at −78 °C with stirring. At this temperature *n*-BuLi (1.6 M in hexanes, 4.0 mL, 6.4 mmol) was added dropwise via syringe. Once the addition was completed, the solution was stirred for 3 h at room temperature. $Me_2SnCl_2$ (0.71 g, 3.2 mmol) dissolved in 15 mL of diethyl ether was then added dropwise via syringe at room temperature and the mixture was stirred overnight. After this period a cloudy solution was obtained and the solvent was removed in vacuo. Hexane was vacuum transferred into the flask, and the milky solution obtained was sonicated for 10 min. The solution was filtered through Celite, and the solvent was removed in vacuo, affording $C_{12}H_8SnMe_2$ as a white solid. Yield: 0.93 g, 96%. Anal. Calcd for $C_{14}H_{14}Sn$: C, 55.87; H, 4.66. Found: C, 55.12; H, 4.67. $^1$H NMR ($C_6D_6$): 0.27 (s, 6 H, $^{117}$Sn (7.7%), and $^{119}$Sn (8.4%) satellites $^2J$ = 57.8 Hz, 60.2 Hz), 7.85 (m, 2 H), 7.53 (m, 2 H), 7.27 (m, 2 H), 7.20 (m, 2 H). $^{13}$C{$^1$H} NMR ($CD_2Cl_2$): 148.79 (s, quaternary), 141.65 (s, quaternary), 136.92 (s, 2 C), 129.67 (s, 2 C), 128.07 (s, 2 C), 122.93 (s, 2 C), −8.27 (s, 2C, $^{117}$Sn (7.7%) and $^{119}$Sn (8.4%) satellites $^1J$ = 348.33 Hz, 364.62 Hz). $^{119}$Sn{$^1$H} NMR ($C_6D_6$): −34.1.

**Synthesis of 9-Phenyl-9-borafluorene, 2.** $C_{12}H_8SnMe_2$ (1.9 g, 6.3 mmol) was placed in a 50 mL flask, and toluene (25 mL) was vacuum transferred into the flask at −78 °C. $C_6H_5BCl_2$ (1.0 g, 6.3 mmol) also dissolved in toluene (10 mL) was added dropwise via syringe at −78 °C. The mixture was slowly warmed to room temperature and stirred overnight. A bright yellow solution was obtained, and after removal of the solvent under vacuum a waxy yellow solid was obtained. The solid was transferred to a sublimator, and the $Me_2SnCl_2$ byproduct was fully removed under static vacuum at 40 °C for 2 days. The yellow solid obtained as a residue contained pure **2** as judged by NMR spectroscopy. Yield: 1.5 g (99%). Anal. Calcd for $C_{18}H_{13}B$: C, 90.08; H, 5.42. Found: C, 85.97; H, 5.67. Carbon analyses were consistently low for this compound. $^1$H NMR ($CD_2Cl_2$): 8.20 (m, 2 H), 7.82 (m, 2 H), 7.65−7.57 (m (overlap), 3 H), 7.46 (m, 2 H), 7.38 (m, 2 H), 7.19 (m, 2 H). $^{13}$C{$^1$H} NMR ($CD_2Cl_2$): 154.9 (s, quaternary), 136.31 (s, 2 C), 135.42 (s, 2 C), 134.67 (s, 2 C), 132.84 (s, 2 C), 128.78 (s (overlap), 4C), 120.37 (s, 2 C). $^{11}$B{$^1$H} NMR ($C_6D_6$): 64.5.

**Synthesis Cp*Al·(1a), 3a.** [Cp*Al]$_4$ (50 mg, 0.31 mmol based on monomer) was suspended in ca. 3 mL of toluene in a vial and stirred for 5 min. **1a** (146 mg, 0.31 mmol) was dissolved in a separate vial in ca. 3 mL of toluene and added dropwise to the stirred suspension of [Cp*Al]$_4$. The yellow-orange solution obtained was stirred for 20 min and then filtered into a vial and layered with hexanes. After cooling overnight at −35 °C, yellow crystals of **3a** were obtained. The crystals were washed with cold hexanes and dried under vacuum. Yield: 99 mg, 50%. Anal. Calcd for $C_{34}H_{15}AlBF_{13}$: C, 52.85; H, 2.36. Found: C, 52.30; H, 2.40. $^1$H NMR ($C_6D_6$): 1.11 (s, 15 H, $C_5(CH_3)_5$). $^{13}$C{$^1$H} NMR ($C_6D_6$): 116.21 (s, $C_5(CH_3)_5$), 8.28 (s, $C_5(CH_3)_5$). $^{11}$B{$^1$H} NMR ($C_6D_6$): −25.4. $^{27}$Al NMR ($C_6D_6$): −114.3. $^{19}$F{$^1$H} NMR ($C_6D_6$): −129.7 (2 F, *o*-F), −133.1 (2 F), −136.1 (2 F), −157 (1 F, *p*-F), −157.7 (2 F), −158.1 (2 F), −162.6 (2F, *m*-F).

**Synthesis of Cp*Al·(1b), 3b.** In the glovebox, [Cp*Al]$_4$ (35 mg, 0.22 mmol based on monomer) was suspended in ca. 2 mL of bromobenzene. In a separate vessel, **1b** (70 mg, 0.22 mmol) was dissolved in bromobenzene and then added dropwise to the suspension of [Cp*Al]$_4$. The yellow-orange suspension obtained was gently heated in a hot plate to dissolve the unreacted Cp*Al and then quickly filtered into a vial to separate insoluble impurities. The clear yellow solution obtained was layered with pentane and cooled at −35 °C overnight. Yellow crystals of **3b** were obtained after 24 h, which were washed with cold pentane and vacuum-dried. Yield: 35 mg, 33%. Anal. Calcd for $C_{23}H_{18}AlBF_8$: C, 57.05; H, 3.72. Found: C, 57.02; H, 3.72. $^1$H NMR ($C_6D_6$): 1.85 (15 H, $C_5(CH_3)_5$), 0.29 (3 H, B−$CH_3$). $^{13}$C{$^1$H} NMR ($C_6D_6$): 115.77 (s, $C_5(CH_3)_5$), 8.48 (s, $C_5(CH_3)_5$). $^{11}$B{$^1$H} NMR ($C_6D_6$): −14.7. $^{27}$Al NMR ($C_6D_6$): −114.3. $^{19}$F{$^1$H} NMR ($C_6D_6$): −135.7 (2 F), −137.0 (2 F), −159.8 (2 F), −160.2 (2 F).

**Synthesis of Cp*Al·(2), 4.** [Cp*Al]$_4$ (68 mg, 0.42 mmol based on monomer) and **2** (100 mg, 0.42 mmol) were mixed in a 50 mL glass bomb in the glovebox, and ca. 5−10 mL of toluene was added at room temperature. A black suspension was obtained because of the formation of metallic aluminum. The vessel was then heated in an oil bath at 60−70 °C for 1 h to dissolve the unreacted [Cp*Al]$_4$. In the glovebox, the solution was filtered directly into a small vial and a clear yellow solution was obtained. The solution was layered with pentane and cooled at −35 °C overnight. Yellow crystals of **4** were obtained after this period. The crystals were washed with cold pentane and dried under vacuum. Yield: 45 mg, 27%. Anal. Calcd for $C_{28}H_{28}AlB$: C, 83.63; H, 6.97. Found: C, 81.05; H, 7.29. Carbon analyses were consistently low for this compound. $^1$H NMR ($C_6D_6$): 8.00−7.98 (m, 2 H), 7.88−7.85 (m, 2 H), 7.77−7.75 (m, 2 H), 7.31−7.25 (m, 6 H), 7.13−7.10 (m, 1 H), 1.19 (s, 15 H, $C_5(CH_3)_5$). $^{13}$C{$^1$H} NMR ($C_6D_6$, 20000 scans): 155.4 (s, br), 146. 0 (s), 135.9 (s), 132.7 (s), 126.4 (s), 126.2 (s), 125.9 (s), 120.8 (s) 115.3 (s), 8.7 (s). $^{11}$B{$^1$H} NMR ($C_6D_6$): −5.0. $^{27}$Al NMR ($C_6D_6$): −70.3.

**Synthesis of $2Li_2{\cdot}(THF)_n$. 2** (300 mg, 1.25 mmol) and an excess of Li powder (44 mg, 5 equiv) were weighed together into a 50 mL round-bottom flask, and the system was connected to a swivel frit in the glovebox. In the vacuum line, THF (20 mL) was vacuum transferred into the flask at −78 °C. The reaction mixture was warmed at room temperature and stirred overnight. The excess lithium powder was separated by filtration from the dark red-brown solution, and the solvent was vacuum evaporated. The pasty solid residue was extracted into toluene (2 × 10 mL) and decanted to remove insoluble impurities. The solution was layered with pentane and cooled at −35 °C overnight to yield dark green crystals. The crystals were washed with cold pentane and dried slowly

(31) Dougherty, T. K.; Lau, K. S. Y.; Hedberg, F. L. *J. Org. Chem.* **1983**, *48*, 5273.
(32) Pangborn, A. B.; Giardello, M. A.; Grubbs, R. H.; Rosen, R. K.; Timmers, F. J. *Organometallics* **1996**, *15*, 1518.

**Table 2. Summary of Data Collection and Structure Refinement Details for Complexes**

| | 3a | 3b | 4 | 5 |
|---|---|---|---|---|
| formula | $C_{41}H_{23}AlBF_{13}$ | $C_{23}H_{18}AlBF_8$ | $C_{28}H_{28}AlB$ | $C_{14}H_{23}AlCl_2O$ |
| fw | 728.32 | 484.16 | 402.29 | 305.20 |
| cryst syst | triclinic | monoclinic | monoclinic | monoclinic |
| *a*, Å | 10.0810(1) | 16.6916(7) | 11.0625(1) | 8.5509(2) |
| *b*, Å | 11.3355(1) | 13.9942(6) | 12.7668(2) | 17.8743(6) |
| *c*, Å | 14.7178(1) | 18.0524(9) | 17.3434(3) | 11.4519(4) |
| α, deg | 100.320(1) | | | |
| *β*, deg | 90.371(1) | 90.647(2) | 108.228(1) | 110.9044(13) |
| *γ*, deg | 108.127(1) | | | |
| *V*, Å$^3$ | 1569.04(2) | 4216.5(3) | 2326.54(6) | 1635.11(9) |
| space group | $P\bar{1}$ | $P2_1/n$ | $P2_1/n$ | $P2_1/n$ |
| *Z* | 2 | 8 | 4 | 4 |
| $d_{calc}$, mg m$^{-3}$ | 1.542 | 1.525 | 1.149 | 1.240 |
| $\mu$, mm$^{-1}$ | 0.17 | 0.18 | 0.099 | 0.44 |
| R1 | 0.043 | 0.093 | 0.044 | 0.052 |
| wR2 | 0.106 | 0.218 | 0.112 | 0.126 |
| wR2 (all data) | 0.117 | 0.228 | 0.126 | 0.149 |
| gof | 1.02 | 1.02 | 1.03 | 1.04 |

at room temperature. Under vacuum, solvent is removed and the crystals become a pasty solid difficult to handle. **2**$Li_2$·$(THF)_n$ crystallizes with a different number of coordinated THF molecules depending on the experimental conditions, with $n = 2-4$. Yield: 50−55%. Anal. Calcd for $C_{26}H_{29}BLi_2O_2$ (2 molecules of THF): C, 78.40; H, 7.29. Found: C, 77.99; H, 7.35. $^1$H NMR ($d_8$-THF): 8.24 (d, 2 H, $^3J_{H-H} = 8.3$ Hz), 8.10 (d, 2 H, $^3J_{H-H} = 7.8$ Hz), 8.01 (d, 2 H, $^3J_{H-H} = 8.1$ Hz), 7.01 (t, 2 H, $^3J_{H-H} = 7.7$ Hz), 6.60−6.54 (m, 3 H), 6.35 (m, 2H), 3.62 (m, variable), 1.79 (m, variable). $^{13}$C{$^1$H} NMR ($C_6D_6$): 135.42 (s, quaternary), 132.64 (s, 2 C), 129.82 (s, 2 C), 127.27 (s, 2 C), 121.07 (s, 2 C), 119.21 (s, 2 C), 118.77 (s, 1 C), 116.53 (s, 2 C), 110.19 (s, 2 C). $^{11}$B{$^1$H} NMR ($d_8$-THF): 6.3.

**Synthesis of Cp*$AlCl_2$·THF, 5.** [Cp*$AlCl_2$]$_2$ (0.58 g, 2.5 mmol based on monomer) was dissolved in 5 mL of toluene in a vial in the glovebox. THF (0.20 mL, 2.5 mmol) was then syringed into the vial, and a pale yellow solution was obtained. The solution was filtered through Celite to eliminate insoluble impurities, and the clear solution obtained was layered with pentane and cooled at −35 °C overnight. Colorless crystals of **5** were obtained after 24 h, which were washed with cold pentane and dried under vacuum. Yield: 0.66 g, 87%. $^1$H NMR ($C_6D_6$): 3.47 (m, 4 H), 1.96 (s, 15 H, $C_5(CH_3)_5$), 0.83 (m, 4 H). $^{13}$C{$^1$H} NMR ($C_6D_6$): 117.53 (s, $C_5(CH_3)_5$), 71.73 (br, O-$CH_2$-$CH_2$), 24.87 (s, $C_5(CH_3)_5$), 11.94 (m, O−$CH_2CH_2$). $^{27}$Al NMR ($C_6D_6$): 82.4.

**Reaction between 2$Li_2$·$(THF)_2$ and 5.** In the glovebox, **2**$Li_2$·$(THF)_2$ (170 mg, 0.427 mmol) and **5** (130 mg, 0.427 mmol) were weighed into a 50 mL round-bottom flask and connected to a swivel frit. In the vacuum line, THF (25 mL) was condensed onto the solids at −78 °C, and the dark brown solution obtained was stirred for 20 min. The system was slowly warmed to room temperature, and at 0 °C the solution presents an intense blue color. After 5 min at room temperature a clear yellow solution was obtained along with appreciable amounts of aluminum metal. The solvent was evaporated to dryness, the residue was extracted into bromobenzene or $CH_2Cl_2$ (10 mL), and the white insoluble solid was filtered along with the aluminum metal. The solvent was removed in vacuo, and NMR analysis indicated the presence of Cp*-H and **2**·(THF) as the main identifiable products.

**Computational Details.** The geometric structures of all borole and 9-borafluorene complexes were optimized at the DFT level of theory, using the B3LYP hybrid functional (comprised of Becke's hybrid exchange functional[33] and the correlation functional of Lee, Yang, and Parr[34]) in conjunction with the 6-31G** basis set.[35] To optimize the geometries of the unstable $\eta^1$-**I**-AlCp and $\eta^5$-**II**-AlCp complexes, it was necessary to fix the $C_\beta-C_\alpha-B-Al$ dihedral angles for $\eta^1$-**I**-AlCp and the $C_\alpha-Al$, $C_\beta-Al$, and $B-Al$ bond distances for $\eta^5$-**II**-AlCp. The Jaguar program[36] was employed for all of the geometry optimization calculations. The ADF package[37] was employed for the fragment orbital analysis calculations. These calculations were carried out at the DFT level of theory with the PBE exchange−correlation functional.[38] The core electrons of all heavy atoms were kept frozen, and a double-ζ slater valence basis set, augmented with a d polarization function on all heavy atoms and a p polarization function on H, was employed. In the fragment orbital analysis calculations the geometries of **I**-AlCp and **II**-AlCp were fixed at their respective B3LYP/6-31G** optimized structures.

**X-ray Crystallography.** Crystal data and refinement details are given in Table 2; full details can be found in the Supporting Information.

**Acknowledgment.** Funding for this work came from the Natural Sciences and Engineering Research Council of Canada in the form of a Discovery Grant, an E. W. R. Steacie Fellowship (2001−2003) (to W.E.P.), and the Province of Ontario in the form of a Premiers' Research Excellence Award (to T.K.W.). Funding for computing resources was provided by the Canadian Foundation for Innovation, the Ontario Innovation Trust Fund, the Natural Sciences and Engineering Research Council of Canada, and the University of Western Ontario Academic Development Fund.

**Supporting Information Available:** Full experimental details concerning the X-ray crystallography, tables of atomic coordinates, anisotropic displacement parameters, and complete bond distances and angles for the structurally characterized molecules are presented. This material is available free of charge via the Internet at http://pubs.acs.org.

OM0209935

(33) Becke, A. D. *J. Chem. Phys.* **1993**, *98*, 5648.
(34) Lee, C.; Yang, W.; Parr, R. G. *Phys. Rev. B* **1988**, *37*, 785.
(35) (a) Harihan, P. C.; Pople, J. A. *Theor. Chim. Acta* **1973**, *28*, 213. (b) Francl, M. M.; Petro, W. J.; Hehre, W. J.; Binkley, J. S.; Gordon, M. S.; DeFrees, D. J.; Pople, J. A. *J. Chem. Phys.* **1982**, *77*, 3654.
(36) *Jaguar 4.1*; Schrodinger, Inc.: Portland, OR, 2000.
(37) *ADF 2002.02*; Scientific Computing and Modeling NV: Amsterdam, The Netherlands, 2002.
(38) Perdew, J. P.; Burke, K.; Ernzerhof, M. *Phys. Rev. Lett.* **1996**, *77*, 3865.